Journal Pre-proofs

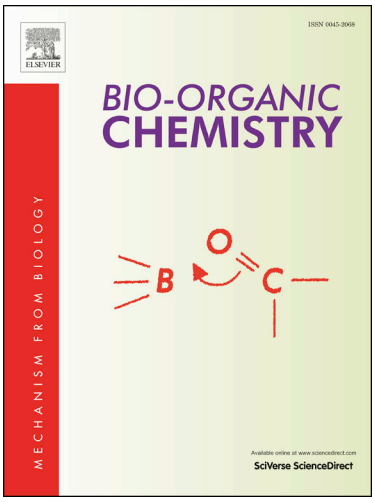

INTERACTIONS OF TOLCAPONE ANALOGUES AS STABILIZERS OF THE AMYLOIDOGENIC PROTEIN TRANSTHYRETIN

Valentina Loconte, Michele Cianci, Ilaria Menozzi, Davide Sbravati, Francesco Sansone, Alessandro Casnati, Rodolfo Berni

PII: S0045-2068(20)31441-3
DOI: https://doi.org/10.1016/j.bioorg.2020.104144
Reference: YBIOO 104144

To appear in: *Bioorganic Chemistry*

Received Date: 26 February 2020
Revised Date: 22 May 2020
Accepted Date: 23 July 2020

Please cite this article as: V. Loconte, M. Cianci, I. Menozzi, D. Sbravati, F. Sansone, A. Casnati, R. Berni, INTERACTIONS OF TOLCAPONE ANALOGUES AS STABILIZERS OF THE AMYLOIDOGENIC PROTEIN TRANSTHYRETIN, *Bioorganic Chemistry* (2020), doi: https://doi.org/10.1016/j.bioorg.2020.104144

INTERACTIONS OF TOLCAPONE ANALOGUES AS STABILIZERS OF THE AMYLOIDOGENIC PROTEIN TRANSTHYRETIN

Valentina Loconte [1, a], Michele Cianci [2, a], Ilaria Menozzi [3], Davide Sbravati [3], Francesco Sansone [3], Alessandro Casnati [3], Rodolfo Berni [3]

[1]iHuman Institute, ShanghaiTech University, 201210 Pudong, Shanghai, China.

[2]Department of Agricultural, Food and Environmental Sciences, Polytechnic University of Marche, 60131 Ancona, Italy.

[3]Department of Chemistry, Life Sciences and Environmental Sustainability, University of Parma, 43124 Parma, Italy.

[a] These authors contributed equally to this work

Correspondence to:

Rodolfo Berni - Parco Area Scienze 23/A, 43124 Parma, Italy

Tel +39-0521905645; Fax +39-0521905151.

E-mail address: rodolfo.berni@unipr.it

ORCID: 0000-0002-1839-0479

Francesco Sansone - Parco Area Scienze 17/A, 43124 Parma, Italy

Tel +39-0521905458; Fax +39-0521905556

E-mail address: francesco.sansone@unipr.it

ORCID: 0000-0003-0531-9865

ABSTRACT

Transthyretin (TTR) is an amyloidogenic homotetramer involved in the transport of thyroxine and retinol in blood and cerebrospinal fluid. TTR stabilizers, such as tolcapone, an FDA approved drug for Parkinson's disease, are able to interact with residues of the thyroxine-binding sites of TTR, both wild type and pathogenic mutant forms, thereby stabilizing its tetrameric native state and inhibiting amyloidogenesis. Herein, we report on the synthesis of 3-deoxytolcapone, a novel stabilizer of TTR. The high-resolution X-ray analyses of the interactions of 3-O-methyltolcapone and 3-deoxytolcapone with TTR were performed. In the two ligand-TTR_complexes the tolcapone analogues establish mainly H-bond and hydrophobic interactions with residues of the thyroxine-binding site of the TTR tetramer. Both compounds are capable of high and selective stabilization of TTR in the presence of plasma proteins, despite their markedly different 'forward' and 'reverse' binding mode, respectively. In fact, the loss or the weakening of stabilizing interactions with protein

residues of 3-deoxytolcapone in comparison with tolcapone and 3-O-methyltolcapone is compensated by new interactions established at the dimer-dimer interface. Our data, coupled with previously reported data on the pharmacokinetics properties in humans of tolcapone and 3-O-methyltolcapone, further support the relevance of the latter tolcapone analogue as TTR stabilizer.

Keywords: Amyloidogenic proteins; Transthyretin; Amyloidogenesis inhibitors; Transthyretin stabilizers; Structure-activity relationships; Tolcapone analogues.

Abbreviations: *TTR, transthyretin; wt TTR, wild type TTR; RBP4, plasma retinol-binding protein; ATTR, TTR-related amyloidosis; T4, thyroxine; HBP, halogen binding pocket; SSA, senile systemic amyloidosis; DCM, dichloromethane; TLC, thin layer chromatography; HPLC, high performance liquid chromatography; PDB, Protein Data Bank.*

Note for figures: color must be used only for print version of the paper

1.Introduction

Peptides and proteins that can produce the accumulation in tissues of highly structured protein aggregates, the amyloid fibrils, are responsible for degenerative diseases known as amyloidoses, generated through an unknown toxic mechanism [1]. Transthyretin (TTR) is an amyloidogenic homotetramer of about 55 kDa involved in the transport of thyroxine (T4) and the co-transport of retinol in blood and cerebrospinal fluid *via* plasma retinol-binding protein [2,3]. Structurally, two TTR monomers are held together to form a stable dimer through a network of H-bond interactions involving the two edge β-strands H and F of each monomer. Two dimers in turn associate to form the tetramer where, at the dimer-dimer interface, a central cavity harboring two funnel-shaped T4 binding sites, coincident with one of the twofold symmetry axes, traverses the entire tetramer [4]. Each pair of twofold-related monomers forms a hormone-binding site, which is lined with two sets of three hydrophobic halogen binding pockets (HBPs), wherein the iodine atoms of bound T4 are accommodated [2]. They are distinguished in an outer binding subsite (HBP 1 and HBP 1'), an inner binding subsite (HBP 3 and HBP 3'), and an intervening interface (HBP 2 and HBP 2'). Regarding the changes that this protein undergoes to give rise to amyloid aggregates, evidence was obtained consistent with the rate-limiting dissociation of the TTR tetramer, followed by misfolding of TTR monomers and their downhill polymerization leading to the formation of amyloid fibrils [5,6]. Both wild type (wt) TTR and the more aggressive amyloidogenic TTR mutants may give rise to the TTR-related amyloidosis (ATTR). Wt TTR possesses in fact an inherent amyloidogenic potential [7], and the associated ATTR, formerly called senile systemic amyloidosis (SSA), is an under-diagnosed disease, which manifests itself in the elderly and is mainly characterized by cardiomyopathy [8]. More than 120 pathologic TTR mutations are responsible for hereditary ATTR, whose main pathological phenotypes are cardiomyopathy and peripheral polyneuropathy [9,10].

Different therapeutic strategies were addressed to date for the treatment of ATTR, in particular liver transplantation, the stabilization of the TTR tetrameric native structure by specific ligands designated TTR stabilizers, and more recent therapies based on TTR specific siRNA and anti-sense oligonucleotides [9,10]. TTR-bound stabilizers establish interactions bridging the couple of monomers that line the T4 binding site, thereby stabilizing the TTR tetrameric native state and inhibiting amyloidogenesis [5,11-15]. Two distinct binding modes characterize TTR stabilizers. The "forward" and "reverse" binding modes refer to the position of the hydrophilic moiety of bound ligands in the outermost or the innermost part of the TTR binding cavity, respectively [16]. Tafamidis (Fig. 1), the only TTR ligand approved to date for the pharmacological therapy of ATTR, was found to delay the disease progression in patients at early stages of ATTR polyneuropathy [17,18] and cardiomyopathy [19]. Tolcapone (Fig. 1), an FDA approved drug for Parkinson's disease, was recently repurposed as a potent and selective TTR stabilizer, possessing an *ex-vivo* anti-amylodogenic activity higher than that of tafamidis. It could be suitable for the treatment of TTR amyloidoses also affecting the central nervous system, owing to its ability to penetrate the brain [20]. On the other hand, the 3-hydroxy substituent

of tolcapone is highly susceptible to glucuronidation, which in humans leads to the rapid elimination of the drug as glucuronidated metabolite[21]. The short half-life in the plasma (about 3 hours) of tolcapone [21] can thus limit its use as TTR stabilizer. On the contrary, 3-O-methyltolcapone (Fig. 1), a minor metabolite of tolcapone generated by the methylation of the aforementioned hydroxy group, represents a long-lived tolcapone metabolite (half-life in the plasma of about 40 hours) [21]. Owing to the close similarity of its chemical structure with that of tolcapone, we hypothesized that it could represent an efficient TTR stabilizer possessing better pharmacokinetics properties in comparison with tolcapone. Better pharmacokinetics relative to tolcapone is also expected for 3-deoxytolcapone (Fig. 1), in which the susceptible 3-hydroxy group substituent in the nitrophenyl ring is lacking, but such compound has never been reported in the literature. We report here on the first synthesis of 3-deoxytolcapone, an *ex-vivo* study of the anti-amyloidogenic potential of 3-O-methyltolcapone and 3-deoxytolcapone, and X-ray analysis of the molecular determinants affecting the ability of the aforementioned tolcapone analogues to effectively and selectively stabilize the TTR tetrameric native structure.

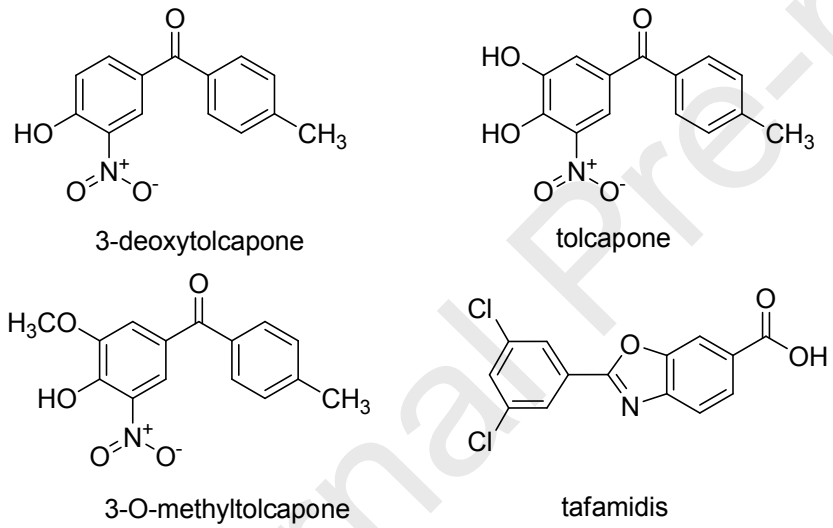

Figure 1. Chemical structures of 3-deoxytolcapone, tolcapone, 3-O-methyltolcapone and tafamidis.

2. Materials and Methods

2.1 Materials

Recombinant human wt TTR was prepared and quantified essentially as described [22]. Tolcapone, tafamidis and 3-O-methyltolcapone were purchased from Carbosynth.

2.2 Synthesis of 3-Deoxytolcapone

The chemical reactions were carried out under nitrogen atmosphere using solvents dried with standard procedures, monitored by Thin Layer Chromatography (TLC) on silica gel 60 F_{254}, using either UV

light (254 nm) or staining agents ($FeCl_3$, green bromocresol) to reveal functional groups. ^1H and ^{13}C-NMR spectra were registered on Bruker AVANCE300 and AVANCE400 spectrometers (^1H 300/400 MHz, ^{13}C 100 MHz) with residual non-deuterated solvent as internal standard. Low-resolution mass spectra were obtained on Waters SQ Detector ESI-MS. Elemental analysis and HPLC analysis were performed by means of a Thermo Fisher FlashSmart Instrument and an Agilent Technologies 1260 Infinity, respectively. Both methods confirmed a purity of the product > 95%. Melting point was determined on a Gallenkamp apparatus in sealed capillary tube in nitrogen atmosphere.

1-(4-Hydroxy-5-nitrophenyl)-1-(4'-methylphenyl)methanone (3-deoxytolcapone): 4-Hydroxy-3-nitrobenzoic acid (5.46 mmol, 1.00 g) and dry DMF (1.31 mmol, 0.102 ml) were dissolved in dry toluene (15 ml) in a two-necked round bottomed flask. Under magnetic stirring, $SOCl_2$ (10.10 mmol, 0.733 ml) was added to the yellow suspension and subsequently, using a condenser, the mixture was heated at 65 °C to get all the reactants more soluble. After 4 hours the solution was quickly cooled down in an ice bath and then dry toluene (2 ml) and dry $AlCl_3$ (12.01 mmol, 1.60 g) were added. The mixture was left reacting overnight at room temperature. After this, the reaction mixture resulted as a viscous brownish oil, which was analyzed by TLC to assess total completion of the reaction (EtOAc/Hex 4/1, Rf=0.51). The oil was treated with aqueous 0.025N HCl (60 ml) and the mixture stirred for 20 min. Once the oil was dissolved and the mixture turned orange, the suspension was filtered and the aqueous layer was extracted with toluene (2×50 ml). The organic layers were combined and basified with 30% NH_3 (5 ml). As the solution turned yellow, the formed solid was filtered and suspended again in 1N HCl (20 ml). After 30 min, the solid was filtered, dissolved in hot DCM and recrystallized at -4 °C to give the title compound as bright yellow crystals (0.78 g, 3.03 mmol, 55%). ^1H NMR (300 MHz, $CDCl_3$) δ (ppm): 10.93 (s, 1H, OH), 8.59 (d, J = 2.0 Hz, 1H, H6), 8.13 (dd, J = 8.7, 2.0 Hz, 1H, H2), 7.70 (d, J = 8.1 Hz, 2H, H2', H6'), 7.34 (d, J = 8.1 Hz, 2H, H3', H5'), 7.32 (d, J = 8.7 Hz, 1H, H3), 2.48 (s, 3H, CH_3). ^{13}C-NMR (100 MHz, $CDCl_3$) δ (ppm): 193.0 (CO), 157.8 (C4), 143.9 (C4'), 138.4 (C2), 134.0 (C5), 132.9 (C1'), 130.3 (C1), 130.0 (C2', C6'), 129.4 (C3', C5'), 127.7 (C6), 120.3 (C3), 21.7 (CH_3). ESI-MS (-): calc. for $C_{14}H_{11}NO_4$: 257.24; found m/z 256.07 [100%, $(M-H)^-$]. Anal. CHNS: calc. for $C_{14}H_{11}NO_4$: C (65.37%), H (4.31%), N (5.45%); found: C (64.99%), H (4.26%), N (5.32%). Mp: 124.8-125.2 °C. HPLC chromatogram and ^1H and ^{13}C NMR spectra of 3-deoxytolcapone are reported in Supplementary Figures 1-3, respectively.

2.3 Western Blot analysis

TTR binding and stability assay in the presence of urea by TTR ligands was conducted for TTR present in human plasma by means of a Western Blot procedure carried out according to a previously reported protocol [23], with some modifications [15], as follows. Aliquots of human plasma were diluted 16 folds in Na phosphate buffer (Na phosphate 40 mM, NaCl 0.15M pH 7.4) and supplemented with 4 and 8 µM of each ligand dissolved in DMSO. One more plasma sample supplemented with DMSO was used as a negative

control. After 2-hour incubation at 20 °C, an equal volume of 8 M urea was added to each sample to obtain a final 4 M urea concentration (final ligand concentrations: 2 and 4 µM). The incubation was prolonged for 18 hours at 20 °C, followed by non-denaturing SDS-PAGE, using Tris-Glycine buffer containing 0.025% SDS in the running buffer and 0.2% SDS in the loading buffer. SDS at these concentrations does not denature TTR tetramers but does prevent re-association of TTR monomers. The blotting step was accomplished by means of a Trans-Blot SD transfer apparatus (BIO-RAD), and the membrane after the blotting step was incubated overnight in blocking buffer containing 5% Skim Milk, at 25 °C. Immunodetection of TTR monomers was performed by employing rabbit anti-human TTR polyclonal Ab (Dako) as primary Ab, and anti-rabbit Ab labeled with Dylight 680 (SERACARE) as secondary Ab. Western Blotting images were recorded by using an Odissey Image System (LI-COR). The employed rabbit anti-TTR antibody does not appear to specifically discriminate between the native fraction of tetrameric TTR distinct from other protein aggregates, and as a consequence only the change in intensity of the band of TTR monomers, which reflects the change in the level of tetrameric TTR dissociation, could be accurately monitored.

2.4 Crystallization, data collection and structure determination

Crystals of wt human TTR in complex with 3-O-methyltolcapone and 3-deoxytolcapone were prepared by co-crystallization by using the hanging-drop vapor diffusion method essentially as described [24]. Human wt TTR (5 mg/ml) in 20 mM sodium phosphate, pH 7, was incubated with a 4-fold molar excess of each tolcapone derivative solubilized in DMSO. Drops (1.5 µl) were formed by mixing equal volumes of the solution containing the TTR-ligand complexes and of the reservoir/precipitant solution (2.2 M ammonium sulfate, 0.1M KCl, 30 mM sodium phosphate, pH 7.0). Single crystals were obtained in about one week of incubation at room temperature. Diffraction data were collected at 100 K using synchrotron radiation at the ID23-2 beamline of the ESRF storage ring, Grenoble (France). Data were processed using XDS [25] and AIMLESS [26]. The crystals of human TTR in complex with 3-O-methyltolcapone and 3-deoxytolcapone belonged to space group $P2_12_12$, isomorphous with most previously determined crystal structures of human TTR, and diffracted to a resolution of 1.21 Å and 1.26 Å, respectively. The two structures were refined starting with a rigid body refinement using REFMAC5 [27] and, as initial model, the crystal structure of TTR in complex with resveratrol-3-O-3-glucuronide (PDB ID: 5AKS) [24] devoid of solvent molecules and ligands, and randomized, to avoid any possible phase bias. Model building and water or ligand addition/inspection were manually conducted using COOT [28]. The structures were refined with *phenix.refine* software within PHENIX suite [29], including the hydrogen atoms in the riding positions.

Atomic coordinates of the ligand molecules and restraints were obtained through the PRODRG server [30] within CCP4 suite [31]. The ligand orientation was determined by inspecting the electron density map,

calculated with (Fo-Fc) coefficients and phases from the model, deprived of the ligand. The final R_{factor} and R_{free} values for TTR in complex with 3-O-methyltolcapone and 3-deoxytolcapone were 0.156 and 0.179, and 0.147 and 0.172, respectively. Models were checked with PROCHECK [32] in the CCP4 suite [31]. Data collection and refinement statistics are reported in Table 1.

TABLE 1. Data collection, processing and refinement statistics*

Data collection	TTR - 3-deoxytolcapone complex (PDB ID: 6SUG)	TTR - 3-O-methyltolcapone complex (PDB ID: 6SUH)
Space group	$P2_12_12$	$P2_12_12$
Unit cell (a, b, c, Å)	43.01; 85.55; 64.52	42.91; 85.46; 64.71
Resolution range (Å)	64.53-1.21 (1.23-1.21)	42.91-1.26 (1.28-1.26)
Total number of reflections	446083 (172773)	382211 (18194)
Unique reflections	72459 (3396)	64681 (3086)
Multiplicity	6.2 (5.1)	5.9 (5.9)
Completeness (%)	98.8 (94.7)	99.6 (98.5)
R_{sym}	0.055 (1.031)	0.086 (1.440)
R_{pim}	0.026 (0.540)	0.058 (0.960)
$\langle I/\sigma(I)\rangle$	15.6 (1.7)	11.1 (2.1)
Refinement statistics		
R_{factor}/R_{free} (%)	0.147/0.172	0.156/0.179
Average all atom B-factor (Å^2)	22.0	21.0
Total number of atoms/water molecules	4282/201	4092/190
Geometry		
Ramachandran favored/allowed/outliers (%)	99.6/0.4/0.0	98.7/1.3/0.0
RMS bonds/angles	0.010/1.170	0.014/1.307

Values in parentheses refer to the highest resolution shell.

3. Results and Discussion

3.1 Synthesis of 3-deoxytolcapone

The synthesis of 3-deoxytolcapone was carried out through a one-pot strategy (Scheme 1). Specifically, 4-hydroxy-3-nitrobenzoic acid was transformed into the corresponding acyl chloride by treatment with $SOCl_2$ and immediately used as reactant in the same round bottomed flask. Toluene, which in the first step was merely a solvent, in the second step acted as a scavenger for acyl chloride intermediate in a Friedel-Crafts reaction. The success of this one-pot reaction was completed by the possibility of easily recrystallizing the desired product. In fact, solubilizing the crude in the minimum amount of boiling dichloromethane followed by a slow cooling, firstly at room temperature and then at -4 °C, it was possible to obtain big rhombic crystals (range 0.5-1 cm) of 3-deoxytolcapone, which were easily filtered.

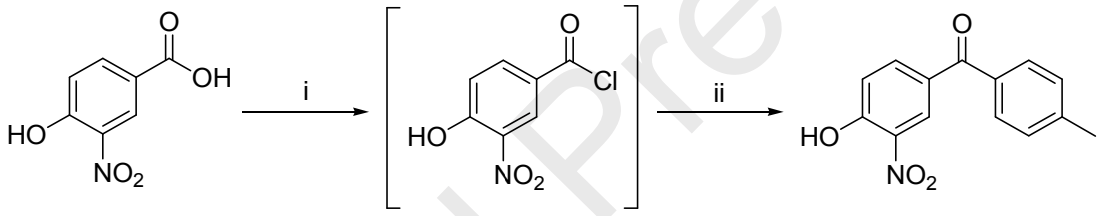

Scheme 1. Synthesis of 3-deoxytolcapone. Reaction conditions: (i) $SOCl_2$ (1.85 eq.), dry DMF (0.24 eq.), dry toluene, 65 °C, 4h; (ii) dry $AlCl_3$ (2.20 eq.), dry toluene, overnight, room temperature, 55% overall yield.

3.2 Comparative analysis of the ability of the tolcapone analogues 3-O-methyltolcapone and 3-deoxytolcapone to selectively stabilize TTR in the presence of plasma proteins

In prospect of using TTR stabilizers for the pharmacological therapy of ATTR, Western Blotting methodologies were developed to evaluate the ability of ligands to interact with TTR, in the presence of the large amount of the other plasma proteins, especially serum albumin. At the same time our Western Blotting analysis provides evidence for the stabilizing effect of tolcapone analogues on the tetrameric native structure of TTR under partially denaturing conditions. Under such conditions (4 M urea), the extent of TTR dissociation, as revealed by the intensity of the band of TTR monomers, is inversely proportional to the ability of TTR ligands to stabilize the tetrameric protein. The comparative analysis of the stabilizing effect of tolcapone and its analogues, along with that of the reference compound tafamidis, was carried out at two ligand concentrations (2 and 4 μM) in diluted human plasma. Indeed, the ability of 3-O-methyltolcapone to

selectively interact with TTR and to protect its native state in the presence of plasma proteins was very high, similar to that of tolcapone, and, remarkably, better than that of tafamidis. The protective effect of 3-deoxytolcapone was also high, and more similar to that of tafamidis as compared to tolcapone and 3-O-methyltolcapone (Fig. 2).

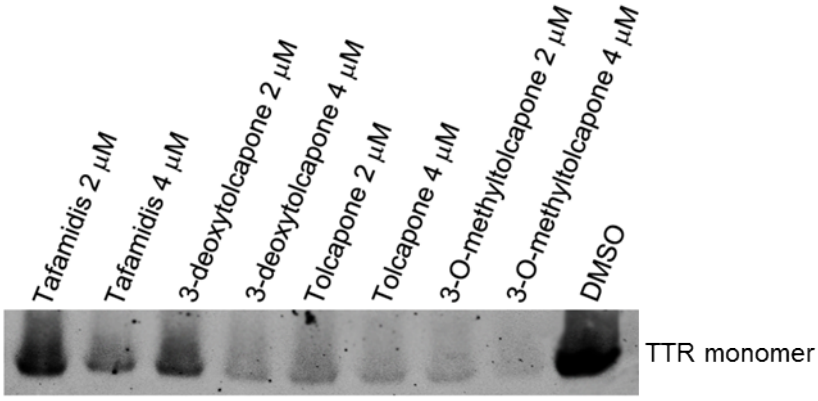

Figure 2. Western Blot analysis of the selective structural stabilization of human plasma TTR by 2 and 4 μM tolcapone, 3-O-methyltolcapone, 3-deoxytolcapone and tafamidis, in the presence of plasma proteins. The intensity of the bands of TTR monomer is inversely proportional to the degree of stabilization of the native tetrameric TTR structure by synthetic ligands in the presence of 4 M urea.

To elucidate the molecular determinants of the stabilizing effect on the TTR tetramer of the two tolcapone analogues and consequently of the inhibition of TTR amyloidogenesis [5,33], the high-resolution X-ray analysis of the structures of their complexes with TTR was performed.

3.3 X-ray structure of wt human TTR in complex with 3-O-methyltolcapone

Based on the X-ray analysis of the structure of the TTR 3-O-methyltolcapone complex, determined at 1.26 Å resolution, the so called 'forward binding mode' was found, which is characterized by the position of the polar moiety of the 3-methoxy-4-hydroxy-5-nitrophenyl ring in the outermost part of the binding cavity (Fig. 3). Such binding mode is the same as that reported for the TTR tolcapone complex [13]. The electron densities for both the 3-methoxy-4-hydroxy-5-nitrophenyl ring and the innermost apolar 4-methyl-phenyl ring are well defined. The r.m.s.d. between equivalent Cα atoms in the monomer of TTR in complex with 3-O-methyltolcapone and tolcapone [13] is 0.484 Å, and the two binding cavities are equally occupied (0.48/0.50). The 4-methyl-phenyl ring of 3-O-methyltolcapone is positioned near the inner hydrophobic binding sites HBP2 and HBP3, deeply into the TTR binding cavity, sitting between Leu110 and Thr119 (Fig. 3b). The central carbonyl group of 3-O-methyltolcapone forms with the OH group of Thr119' at 2.7 Å away a relevant H-bond which is also established by tolcapone within the same distance [13]. The 3-methoxy-4-hydroxy-5-nitrophenyl ring is also held in place by hydrophobic interactions with Leu17/Leu17', Ala108/Ala108', and Val121/Val121', in analogy with the TTR-tolcapone complex. Moreover, the 3-methoxy

group also participates in hydrophobic interactions, namely with Leu17, Val121' and Thr106', enforcing the dimer-dimer interactions that stabilize the TTR tetramer. At variance with the hydrophobic interactions established by the 3-methoxy group, in the TTR-tolcapone complex the 3-hydroxy group can contribute to the stabilization of the TTR tetramer *via* polar interactions [13]. The ε-amino group of Lys15' is sandwiched between the 4-hydroxy and 5-nitro groups of 3-O-methyltolcapone within H-bond distance (2.9 and 3.0 Å, respectively), and Glu54' at 3.0 Å away, in a fashion similar to that described for the TTR-tolcapone complex. However, in the case of the TTR-tolcapone complex Lys15 is sandwiched between the two hydroxy groups of the 3-hydroxy-4-hydroxy-5-nitrophenyl ring, at distances of 3.0 Å, 2.6 Å, and the carboxyl group of Glu54 at 2.9 Å [13].

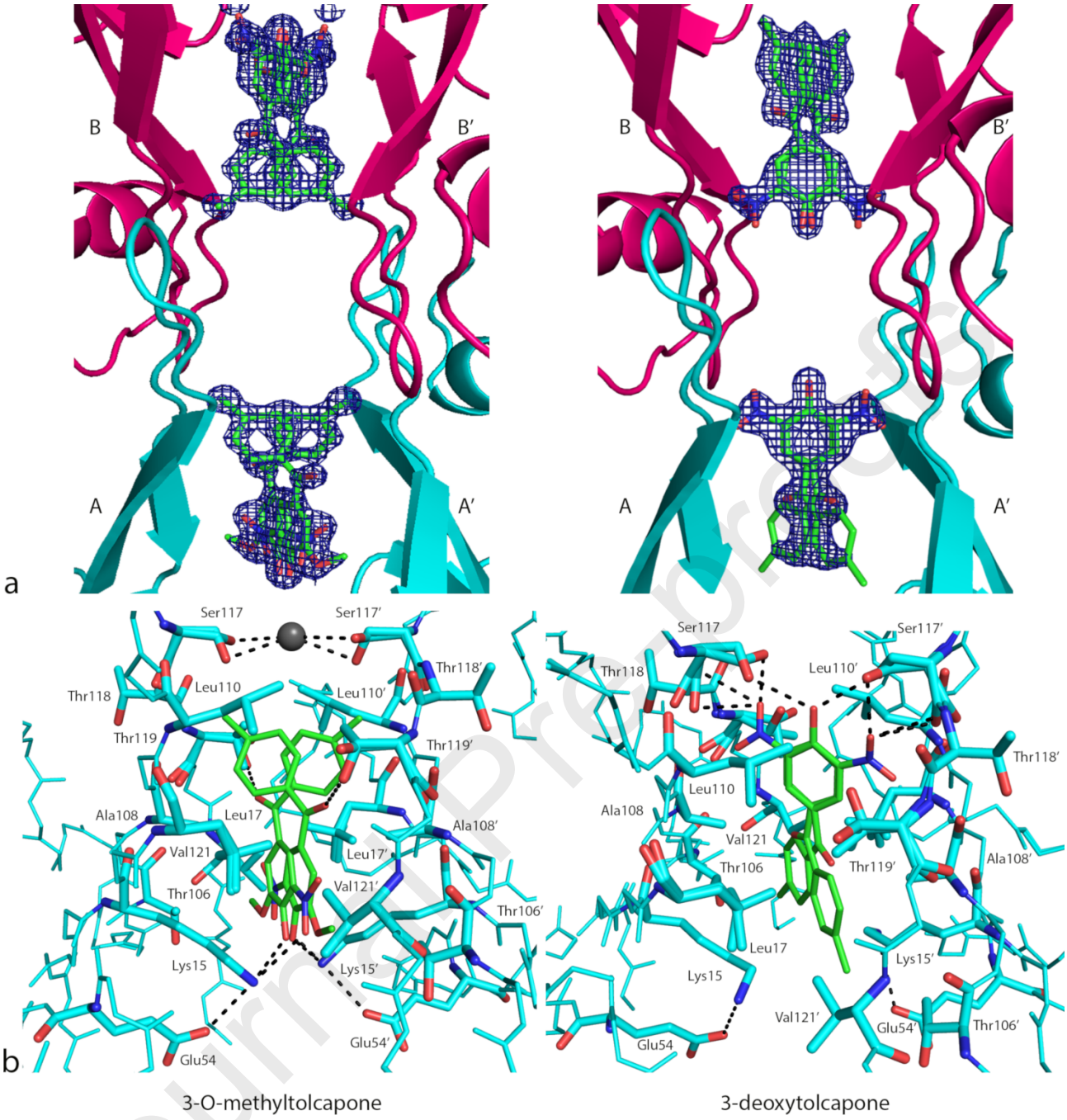

Figure 3. Details of TTR-ligand interactions in the crystal structures of the TTR3-O-methyltolcapone (PDB ID: 6SUH) and TTR3-deoxytolcapone (PDB ID: 6SUG) complexes. a) OMIT (Fo-Fc) electron density maps (blue), contoured at 2.5 σ, of tolcapone analogues (left: 3-O-methyltolcapone; right: 3-deoxytolcapone) bound in the two cavities of the TTR tetramer. b) Detailed views of the two symmetry-related binding modes of each ligand (green) within the T4 binding cavity interacting through residues present in HBP1 (Lys15, stabilized through the interaction with Glu54, and Thr106), HBP2 (Leu110, Leu17, Lys15), and HBP3 (Ser117, Leu110, Ala108, and Thr119). Interacting residues are represented as sticks. A central water molecule (dark gray sphere) establishes hydrogen bond interactions with Ser117 and Ser117' at the dimer-dimer interface of the TTR-3-O-methyltolcapone complex.

The presence of the 2-fold axis along the binding pocket creates two symmetrical binding modes of the ligand, related by a 180° rotation. This situation probably causes the presence of several alternate conformations of the residues in the proximity of 3-O-methyltolcapone, namely Leu17, Ser 117, and Thr119, in analogy with previous observations reported for the TTR-tolcapone complex [13]. Finally, a similar interaction pattern between TTR-bound 3-O-methyltolcapone and tolcapone is also confirmed by the presence of a well conserved network of water molecules, mainly localized at the top and bottom gates of the binding cavity, which are sealed by the presence of Lys15/Glu54 and Ser117 residues, respectively (Fig. 3b).

3.4 X-ray structure of wt human TTR in complex with 3-deoxytolcapone

Unexpectedly, the limited change in the tolcapone molecule consisting in the lack of the hydroxy group at position 3 of the hydrophilic aryl ring, led to a drastic change in the mode of binding of 3-deoxytolcapone as compared to tolcapone. In fact, the structure of TTR in complex with 3-deoxytolcapone, determined at 1.21 Å resolution, reveals the "reverse binding mode" of the ligand (Figs. 3 and 4), with the hydrophilic 4-hydroxy-5-nitrophenyl ring innermost, as opposed to the 'forward binding mode' of bound tolcapone and 3-O-methyltolcapone. Nevertheless, the structure of protein moiety is not significantly affected by the different bound ligands (r.m.s.d.: TTR 3-deoxytolcapone/TTR 3-O-methyltolcapone 0.079 Å; TTR 3-deoxytolcapone/TTR tolcapone 0.503 Å). The electron densities for both the 4-hydroxy-5-nitrophenyl ring and the outermost apolar 4-methyl-phenyl ring are well defined. 3-Deoxytolcapone is bound within the two cavities of the TTR tetramer with nearly the same occupancy (0.47/0.50). In the case of uncomplexed TTR (PDB 1F41) [4] and of the TTR 3-O-methyltolcapone complex (Fig. 3b), a central water molecule establishes H-bonds with the two symmetry-related Ser117/Ser117' residues, thereby bridging the two adjacent monomers at the dimer-dimer interface; on the other hand, in the case of the TTR 3-deoxytolcapone complex H-bond interactions with both Ser117 residues are established by the 4-hydroxy group of the nitrophenyl ring (Fig. 3b). In fact, in the 'reverse binding mode' the 4-hydroxy group is placed within H-bond distance from Ser117 and Ser117' (2.9 Å for both residues). A similar binding geometry was also reported for the potent TTR stabilizer AG10, where the TTR tetramer is stabilized by the presence of H-bonds between the 3,5-dimethyl-1H-pyrazole ring of AG10 and Ser117/Ser117' residues [12]. The nitro group of the nitrophenyl ring of 3-deoxytolcapone is tethered by H-bonds with the OH group of Ser117 at 2.9 Å and with the carbonyl and amide groups of the Thr118-Ser117 peptide bond at 3.3 and 3.2 Å, respectively (Fig. 3b). The 4-methyl-phenyl ring of 3-deoxytolcapone sits in between the outer hydrophobic binding sites HBP1 and HBP1', sandwiched between the aliphatic moieties of the side chains of Lys15/Lys15' and Thr106/Thr106', and the apolar side chains of Ala108/Ala108'and Val121/Val121'. Several residues, namely Leu17, Ser117, Ser115, which are in the proximity of 3-deoxytolcapone, present alternate conformations.

Differently from TTR-bound tolcapone and 3-O-methyltolcapone, the central carbonyl group of 3-deoxyltolcapone is located within a distance of 4.1 Å from the hydroxy group of Thr119 (Fig. 3b) and the ligand shows a rotation of 33° and 29° relative to tolcapone and 3-O-methyltolcapone, respectively (Fig. 3b and 4). Moreover, the lack of the hydroxy substituent in 3-deoxytolcapone allows for a deeper penetration of the ligand of 1.42 Å, as compared to 3-O-methyltolcapone, induced by the reduced steric hindrance and the different ligand binding orientation.

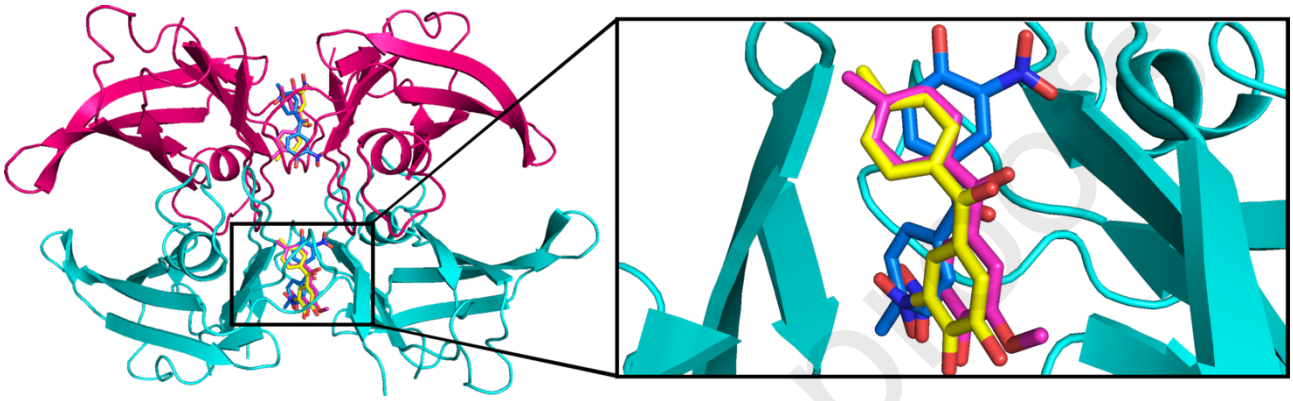

Figure 4. Close-up views of the superimposition of: TTR-3-O-methyltolcapone (magenta) with TTR-tolcapone (yellow), and TTR-3-deoxytolcapone (azure) complexes. The figure shows the displacement of the TTR-bound 3-deoxytolcapone relative to bound tolcapone and 3-O-methyltolcapone, and its rotation, allowing the interaction of the ligand 4-hydroxy group with the Ser117/Ser117' hydroxy groups.

4. Conclusions

In summary, 3-O-methyltolcapone selectively stabilizes the TTR tetramer at the dimer-dimer interface to an extent similar to that of tolcapone, in agreement with the very similar chemical structures of the two ligands and the limited differences in their interactions with TTR. However, the pharmacokinetics of 3-O-methyltolcapone in humans was reported to be remarkably more favorable than that of tolcapone [21]. The lack of a third substituent, either hydroxy or methoxy group, in the nitro-phenyl ring of 3-deoxytolcapone, and, consequently, of its interaction with the protein moiety, leads to the 'reverse binding mode' of this compound (Fig. 3 and 4) and to its significant rotation within the binding cavity. In addition, the reduced steric hindrance of the nitro-phenyl ring allows for a deeper penetration of 3-deoxytolcapone into the TTR binding pocket. Despite its distinct binding mode, 3-deoxytolcapone affords an effective and selective stabilization of TTR in the presence of plasma proteins. In fact, the loss or the weakening of stabilizing interactions with protein residues as compared to tolcapone and 3-O-methyltolcapone is compensated by new interactions established by 3-deoxytolcapone at the dimer-dimer interface. Moreover, the lack of the metabolically susceptible 3-hydroxy group in the nitro-phenyl ring is also expected to significantly increase

the plasma half-life of 3-deoxytolcapone relative to tolcapone. The chemical modification of the 3-hydroxy group or the lack of this group in 3-O-methyltolcapone and 3-deoxytolcapone, respectively, results in a greater lipophilicity of the two tolcapone analogues in comparison with tolcapone. This feature might increase brain permeability and therefore be advantageous for the pharmacological therapy of TTR amyloidoses affecting the central nervous system (leptomeningeal and oculo-leptomeningeal amyloidoses). Based on the scaffold of tolcapone and on the structure-activity relationships of tolcapone analogues, our results provide hints for the design of new effective TTR stabilizers.

Declaration of competing interest

The authors declare that they have no known competing financial interests or personal relationships that could have appeared to influence the work reported in this paper.

Acknowledgments **-** X-ray data collection was performed on the beamline ID23-2 at the European Synchrotron Radiation Facility (ESRF), Grenoble, France, under beamtime allocation proposal MX-1949. We are grateful to Dr Max Nanao at the ESRF for providing assistance in using the beamline ID23-2. We thank Erasmo Neviani for the use of the Odissey Image System.

Funding information - This work received financial support from: Universities of Parma and Marche, Italy, and PRIN Projects (Progetti di Rilevante Interesse Nazionale) 2012A7LMS3_002 and 2017E44A9P of the Italian Ministry of Education, University and Research (MIUR, Rome, Italy). This work also benefited from the equipment and framework of the COMP-HUB initiative by the Departments of Excellence Program 2018-2022 (MIUR, Rome, Italy).

References

[1] F. Chiti, C.M. Dobson, Protein misfolding, amyloid formation, and human disease: a summary of progress over the last decade, Annu. Rev. Biochem. 20 (2017) 27-68. https://doi.org/10.1146/annurev-biochem-061516-045115.

[2] A. Wojtczak, V. Cody, J.R. Luft, W. Pangborn, Structures of human transthyretin complexed with thyroxine at 2.0 angstrom resolution and 3',5'-dinitro-N-acetyl-l-thyronine at 2.2 angstrom resolution, Acta Crystallogr. D Biol. Crystallogr. 52 (1996) 758–765. https://doi.org/10.1107/S0907444996003046.

[3] G. Zanotti, R. Berni, Plasma retinol-binding protein: structure and interactions with retinol, retinoids, and transthyretin, Vitam. Horm. 69 (2004) 271–295. https://doi.org/10.1016/S0083-6729(04)69010-8.

[4] A. Hörnberg, T. Eneqvist, A. Olofsson, E. Lundgren, A.E. Sauer-Eriksson, Comparative analysis of 23 structures of the amyloidogenic protein transthyretin, J. Mol. Biol. 302 (2000) 649–669. https://doi.org/10.1006/jmbi.2000.4078.

[5] S. Connelly, S. Choi, S.M. Johnson, J.W. Kelly, I.A. Wilson, Structure-based design of kinetic stabilizers that ameliorate the transthyretin amyloidoses, Curr. Opin. Struc. Biol. 20 (2010) 54-62. https://doi.org/10.1016/j.sbi.2009.12.009.

[6] M. Schmidt, S. Wiese, V. Adak, J. Engler, S. Agarwal, J. Fritz, P. Westermark, M. Zacharias, M., Fändrich, Cryo-EM structure of a transthyretin-derived amyloid fibril from a patient with hereditary ATTR amyloidosis, Nat. Commun. 10 (2019) 5008. https://doi.org/10.1038/s41467-019-13038-z.

[7] L. Cendron, A. Trovato, F. Seno, C. Folli, A. Alfieri, G. Zanotti, R. Berni, Amyloidogenic potential of transthyretin variants: insights from structural and computational analyses, J. Biol. Chem. 284 (2009) 25832–25841. https://doi.org/10.1074/jbc.M109.017657.

[8] N.J. Galant, P. Westermark, J.N. Higaki, A. Chakrabartty, Transthyretin amyloidosis: an under-recognized neuropathy and cardiomyopathy, Clin. Sci. 131 (2017) 395-409. https://doi.org/10.1042/CS20160413.

[9] M.A. Gertz, M.L. Mauermann, M. Grogan, T. Coelho, Advances in the treatment of hereditary transthyretin amyloidosis: A review. Brain Behav. 9 (2019) e01371. https://doi.org/10.1002/brb3.1371.

[10] A.V. Kristen, S. Ajroud-Driss, I. Conceição, P. Gorevic, T. Kyriakides, L. Obici, Patisiran, an RNAi therapeutic for the treatment of hereditary transthyretin-mediated amyloidosis. Neurodegener. Dis. Manag. 9 (2019) 5-23. https://doi.org/10.2217/nmt-2018-0033.

[11] C.E. Bulawa, S. Connelly, M. DeVit, L. Wang, C. Weigel, J.A. Fleming, J. Packman, E.T. Powers, R.L. Wiseman, T.R. Foss, I.A. Wilson, J.W. Kelly, R. Labaudiniere, Tafamidis, a potent and selective transthyretin kinetic stabilizer that inhibits the amyloid cascade, Proc. Natl. Acad. Sci. USA 109 (2012**)** 9629–9634. https://doi.org/10.1073/pnas.1121005109.

[12] S.C. Penchala, S. Connelly, Y. Wang, M.S. Park, L. Zhao, A. Baranczak, I. Rappley, H. Vogel, M. Liedtke, R.M. Witteles, E.T. Powers, N. Reixach, W.K. Chan, I.A. Wilson, J.W. Kelly, I.A. Graef, M.M. Alhamadsheh, AG10 inhibits amyloidogenesis and cellular toxicity of the familial amyloid cardiomyopathy-associated V122I transthyretin. Proc. Natl. Acad. Sci. USA 110 (2013) 9992–9997. https://doi.org/10.1073/pnas.1300761110.

[13] R. Sant'Anna, P. Gallego, L.Z. Robinson, A. Pereira-Henriques, N. Ferreira, F. Pinheiro, S. Esperante, I. Pallares, O. Huertas, M.R. Almeida, N. Reixach, R. Insa, A. Velazquez-Campoy, D. Reverter, N. Reig, S. Ventura, Repositioning tolcapone as a potent inhibitor of transthyretin amyloidogenesis and associated cellular toxicity, Nat. Commun. 7 (2016) 10787. https://doi.org/10.1038/ncomms10787.

[14] G. Verona, P.P. Mangione, S. Raimondi, S. Giorgetti, G. Faravelli, R. Porcari, A. Corazza, J.D. Gillmore, P.N. Hawkins, M.B. Pepys, G.W. Taylor, V. Bellotti, Inhibition of the mechano-enzymatic amyloidogenesis of transthyretin: role of ligand affinity, binding cooperativity and occupancy of the inner channel. Sci. Rep. 7 (2017) 182. https://doi.org/10.1038/s41598-017-00338-x.

[15] V. Loconte, I. Menozzi, A. Ferrari, C. Folli, B.P. Imbimbo, G. Zanotti, R. Berni, Structure-activity relationships of flurbiprofen analogues as stabilizers of the amyloidogenic protein transthyretin, J. Struct. Biol. 208 (2017) 165-173. https://doi.org/10.1016/j.jsb.2019.08.011.

[16] S.L. Adamski-Werner, S.K. Palaninathan, J.C. Sacchettini, J.W. Kelly, Diflunisal analogues stabilize the native state of transthyretin. Potent inhibition of amyloidogenesis, J. Med. Chem. 47 (2004) 355-374. DOI: 10.1021/jm030347n

[17] M. Waddington Cruz, L. Amass, D. Keohane, J. Schwartz, H. Li, B. Gundapaneni, Early intervention with tafamidis provides long-term (5.5-year) delay of neurologic progression in transthyretin hereditary amyloid polyneuropathy, Amyloid 23 (2016) 178-183. https://doi.org/10.1080/13506129.2016.1207163.

[18] D. Keohane, J. Schwartz, B. Gundapaneni, M. Stewart, L. Amass, Tafamidis delays disease progression in patients with early stage transthyretin familial amyloid polyneuropathy: additional supportive analyses from the pivotal trial, Amyloid 24 (2017) 30-36. https://doi.org/10.1080/13506129.2017.1301419

[19] M.B. Sultan, B. Gundapaneni, J. Schumacher, J.H. Schwartz, Treatment With Tafamidis Slows Disease Progression in Early-Stage Transthyretin Cardiomyopathy, Clin. Med. Insights Cardiol. 11 (2017) 1179546817730322. https://doi.org/10.1177/1179546817730322.

[20] H. Russ, T. Muller, D. Woitalla, A. Rahbar, J. Hahn, W. Kuhn, Detection of tolcapone in the cerebrospinal fluid of parkinsonian subjects, Naunyn-Schmiedeberg's Arch Pharmacol 360 (1999) 719–720. DOI:10.1007/s002109900168

[21] K. Jorga, B. Fotteler, P. Heizmann, R. Gasser, Metabolism and excretion of tolcapone, a novel inhibitor of catechol-O-methyltransferase, Br. J. Clin. Pharmacol. 48 (1999) 513-520. https://doi.org/10.1046/j.1365-2125.1999.00036.x.

[22] N. Pasquato, R. Berni, C. Folli, B. Alfieri, L. Cendron, G. Zanotti, Acidic pH-induced conformational changes in amyloidogenic mutant transthyretin, J. Mol. Biol. 366 (2007) 711-719. https://doi.org/10.1016/j.jmb.2006.11.076.

[23] L. Nilsson, A. Larsson, A. Begum, I. Iakovleva, M. Carlsson, K. Brännström, A.E. Sauer-Eriksson, A. Olofsson, Modifications of the 7-Hydroxy Group of the transthyretin ligand luteolin provide mechanistic insights into its binding properties and high plasma specificity, PLoS One 11 (2016) e0153112. https://doi.org/10.1371/journal.pone.0153112.

[24] P. Florio, C. Folli, M. Cianci, D. Del Rio, G. Zanotti, R. Berni, Transthyretin Binding Heterogeneity and Anti-amyloidogenic Activity of Natural Polyphenols and Their Metabolites, J. Biol. Chem. 290 (2015) 29769-29780. https://doi.org/10.1074/jbc.M115.690172.

[25] W. Kabsch, Acta Crystallogr. D Biol. Crystallogr. 66 (2010) 125–132. https://doi.org/10.1107/S0907444909047337.

[26] P. Evans, Scaling and assessment of data quality. Acta Crystallogr. D Biol. Crystallogr. 62 (2006) 72–82. https://doi.org/10.1107/S0907444905036693.

[27] G.N. Murshudov, P. Skubak, A.A. Lebedev, N.S. Pannu, R.A. Steiner, R.A. Nicholls, M.D. Winn, F. Long, A.A. Vagin, REFMAC5 for the refinement of macromolecular crystal structures, Acta Cryst. D Biol. Crystallogr. 67 (2011) 355-367. https://doi.org/10.1107/S0907444911001314.

[28] P. Emsley, K. Cowtan, COOT: model-building tools for molecular graphics, Acta Crystallogr. D Biol. Crystallogr. 60 (2004) 2126–2132. https://doi.org/10.1107/S0907444904019158.

[29] P.D. Adams, P.V. Afonine, G. Bunkoczi, V.B. Chen, W. Davis, N. Echols, J. Jeffrey, J.J. Headd, L.W. Hung, G.J. Kapral, R.W. Grosse-Kunstleve, A.J. McCoy, N.W. Moriarty, R. Oeffner, R.J. Read, D.C. Richardson, J.S. Richardson, T.C. Terwilliger, P.H. Zwart, PHENIX: a comprehensive Python-based system for macromolecular structure solution, Acta Cryst. D Biol. Crystallogr. 66 (2010) 213-221. https://doi.org/10.1107/S0907444909052925.

[30] A.W. Schüttelkopf, D.M.F. van Aalten, PRODRG: a tool for high-throughput crystallography of protein-ligand complexes, Acta Cryst. D Biol. Crystallogr. 60 (2004) 1355–1363.

[31] M.D. Winn, C.C. Ballard, K.D. Cowtan, E.J. Dodson, P. Emsley, P.R. Evans, R.M. Keegan, E.B. Krissinel, A.G. Leslie, A. McCoy, S.J. McNicholas, G.N. Murshudov, N.S. Pannu, E.A. Potterton, H.R. Powell, R.J.

Read, A. Vagin, K.S. Wilson, Overview of the CCP4 suite and current developments, Acta Crystallogr. D Biol. Crystallogr. 67 (2011) 235–242. https://doi.org/10.1107/S0907444910045749.

[32] R.A. Laskowski, M.W. MacArthur, D.S. Moss, J.M. Thornton, PROCHECK: a program to check the stereochemical quality of protein structures, J. Appl. Cryst. 26 (1993) 283-291. https://doi.org/10.1107/S0021889892009944.

[33] M. Miller, A. Pal, W. Albusairi, H. Joo, B. Pappas, M.T. Haque Tuhin, D. Liang, R. Jampala, F. Liu, J. Khan, M. Faaij, M. Park, W. Chan, I. Graef, R. Zamboni, N. Kumar, J. Fox, U. Sinha, M. Alhamadsheh, Enthalpy-Driven Stabilization of Transthyretin by AG10 Mimics a Naturally Occurring Genetic Variant That Protects from Transthyretin Amyloidosis, J. Med. Chem. 61 (2018) 7862-7876. https://doi.org/10.1021/acs.jmedchem.8b00817.

Highlights

- Inhibitors of TTR amyloidogenesis stabilize the native protein structure
- Tolcapone analogues afford high TTR stabilization
- Crystal structures of TTR in complex with tolcapone analogues have been determined
- Structure-activity relationships of tolcapone analogues have been established